Modeling Convective Instability in FEMLAB

Report Author

Michael Harrison

Chem E 499

Spring 2003

06/11/03

Research Supervisor

Bruce A. Finlayson

Rehnberg Professor of Chemical Engineering

University of Washington

Table of Contents

Introduction

Purpose

The purpose of this research is to determine if convective instability can be modeled using the software package FEMLAB.

Objectives

This research has four main objectives. First, a 2-dimensional simulation is set up in FEMLAB where two infinitely long horizontal plates run parallel to each other. The bottom boundary is maintained at a constant hot temperature, and the top is maintained at a constant cold temperature.

Second, the simulation is set up so that the Incompressible Navier-Stokes equation and the Convection and Conduction equation are solved simultaneously for several values of the Rayleigh number above and below the critical value for this situation.

Third, the results are tabulated. Specifically, the Nusselt number is calculated for each Rayleigh number.

Fourth, a plot of Nusselt number versus Rayleigh number is constructed and compared to theoretical expectations and experimental results. If the plot obtained from FEMLAB agrees with the plot of experimental data, and they both show the same value for the critical Rayleigh number as predicted by theory, then it is safe to conclude that FEMLAB can indeed model convective instability.

Problem Description

The problem to be solved is given schematically in Figure 1.

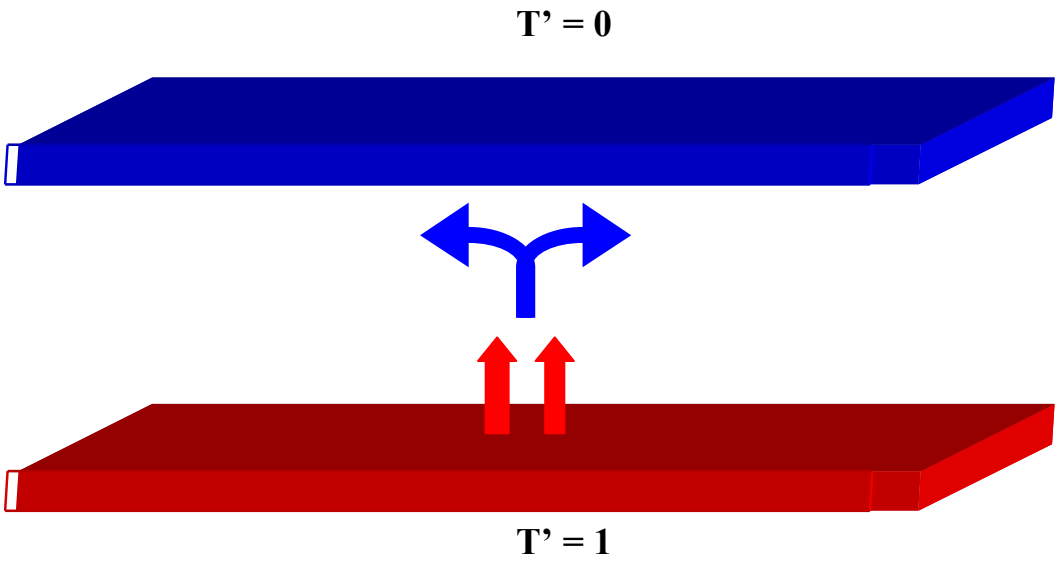

Figure 1. A temperature drop is maintained between two infinitely long plates with fluid filling the space between them. When the temperature drop is great enough, buoyancy forces overcome viscous drag forces. The warm fluid will rise, and the cold fluid will sink. At this point, the system has become unstable, and convection occurs.

The bottom plate is maintained at a constant hot temperature while the top plate is maintained at a constant cold temperature. Initially, heat is transferred by conduction up through the fluid from the bottom plate to the top plate. The hot fluid near the bottom expands and becomes less dense. If the temperature difference is made large enough, the buoyancy forces overcome the viscous drag forces. The hot fluid rises to the top, and the cold fluid sinks to the bottom. Then, that cold fluid heats up, expands, and rises. Thus, the convective movement continues as long as the driving force remains.

Background

This research is inspired by an article from the February 2003 edition of Physics Today[1]. Dr. Albert Libchaber and one of his postdoc students, Dieter Braun, found that an infrared laser pointed at the bottom of a container of a well-mixed dilute DNA solution could create thermally-driven convective flows if the container was of sufficient size. The flow pattern generated by the thermal gradient piled most of the DNA on the bottom and the rest of it in a ring-like pattern in

the middle of the container. Using this method, the concentration of DNA increased by a factor of more than 1000 in some parts of the container.

Theory

The equations necessary to study this problem include the Incompressible Navier-Stokes equation

$$\rho u \bullet \nabla u = -\nabla p + \rho g + \mu \nabla^2 u$$

and an energy equation,

$$\rho C_p u \bullet \nabla T = k \nabla^2 T$$

which is known as the Convection and Conduction equation in FEMLAB. The equations are non-dimensionalized so that the appropriate coefficients can be entered into FEMLAB. The dimensionless forms are

$$\sqrt{Gr}\, u' \bullet \nabla' u' = -\nabla' P' + \sqrt{Gr}\, g_{eff} T' + \nabla'^2 u'$$

and

$$\mathrm{Pr} \sqrt{Gr}\, u' \bullet \nabla' T' = \nabla'^2 T'$$

where primed variables represent dimensionless quantities. P represents the new pressure that takes into account static pressure as well as gravitational forces[2]

$$\nabla P = \nabla p - \rho_o g$$

The Grashoff number is defined as the ratio of buoyancy forces to viscous forces

$$Gr = \frac{\rho^2 \beta_T g \Delta T L^3}{\mu^2}$$

$$\sqrt{Gr} = \left(\frac{\rho}{\mu}\right)\left(\beta_T g \Delta T\right)^{1/2} L^{3/2}$$

and the Prandtl number is defined as the ratio of momentum and thermal diffusivities

$$\Pr = \frac{C_p \mu}{k}$$

The Rayleigh number is related to Prandtl and Grashoff numbers by

$$Ra = \Pr Gr$$

For the details of the derivation of the dimensionless forms, see Appendix A, Section 1. As the temperature difference between the plates increases, the Grashoff number and the Rayleigh number both increase. When the temperature difference is great enough, the critical Rayleigh number Ra_c is reached. Once Ra_c is achieved, convection occurs.

The convective instability problem can be solved analytically, but the equations must be solved simultaneously. It is an eigenvalue problem where the first eigenvalue corresponds to the solution where Ra_c is 1707.762 for the case of rigid boundaries on the top and bottom[3]. This physical situation is the case being studied in this research. For comparison, the Ra_c for the case of a rigid bottom surface and a free top surface, the situation most easily realized in the laboratory, is 1100.6. Ra_c for the case where all surfaces are free is 657.51.

The case of a rigid bottom surface and a free top surface was studied by Benard. After the onset of convection, the top layer of the fluid formed a stable hexagonal cell structure as shown in Figure 1. The structure is caused by gradients in surface tension.

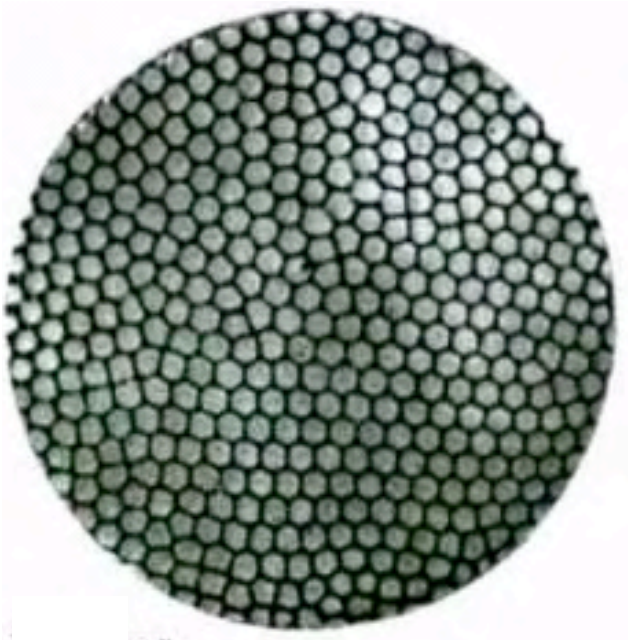

Figure 2. Top view of Benard cells in spermaceti. He discovered the hexagonal cell structure in the early 20th century. He originally studied molten wax[4].

The hexagonal cell structure is the most efficient structure for converting the free energy of the system into the kinetic energy needed for convection. From this point of view, the hexagonal structure is similar to a heat engine that converts unorganized heat into useful work[5].

The Nusselt number is the total non-dimensional heat flux leaving the bottom surface and entering the top surface. It is defined as

$$Nu = \frac{hD}{k}$$

Before the onset of convection, Nu is always equal to one because conduction dominates. Once Ra is greater than Ra_c, Nu will begin to increase and convection heat transfer will also become important. Thus, the onset of convection in FEMLAB can be determined by watching the Nusselt number.

Expectations

The results from FEMLAB are compared to experimentally determined curves. The data of Silveston, Mull, and Reiher are provided in Figure 3.

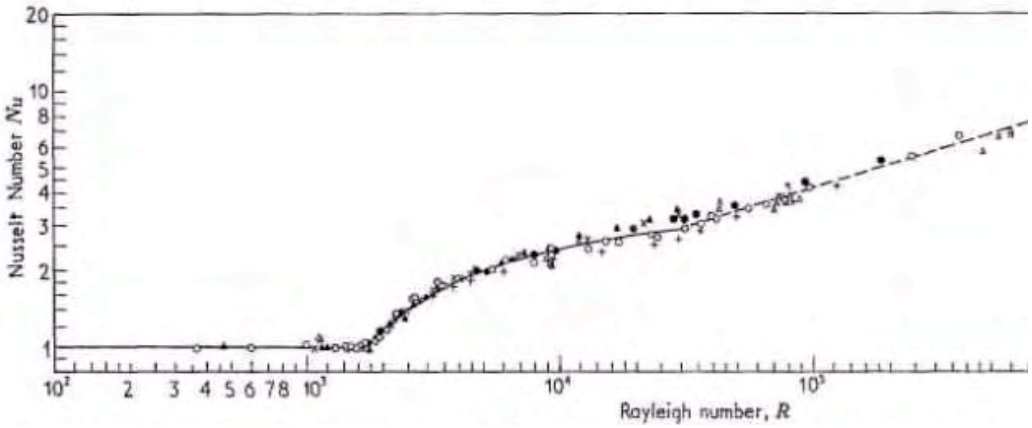

Figure 3. Experimental curve of Nusselt versus Rayleigh number for six different fluids. The Nusselt number is constant at one until the onset of convection around a Rayleigh number of Ra = 1700 $\pm$ 51 (statistically determined by Silveston)[4].

Once convection begins, Nu increases with a square-root shape until becoming somewhat linear (on average) for large Ra values. According to theory, a value for Ra_c of 1707.762 should be expected if FEMLAB is capable of modeling this problem.

Materials and Methods

The software package FEMLAB version 2.3.0.148 is used within Matlab. Microsoft Excel for Windows 97 is used to compute numerical values and plot the data.

Simulation Set-up Procedure

The Boundary and Subdomain settings for each equation are provided below as well as the additional steps that must be taken to achieve the desired results.

First, each equation is divided by its relevant dimensionless variables. This step enhances the convergence of the solution in FEMLAB. For all simulations, the value of g_{eff} is chosen to be one. Thus, the equations now read

$$u' \bullet \nabla' u' = -\frac{1}{\sqrt{Gr}} \nabla' P' + T' + \frac{1}{\sqrt{Gr}} \nabla'^2 u'$$

and

$$u' \bullet \nabla' T' = \frac{1}{\Pr \sqrt{Gr}} \nabla'^2 T'$$

For the Incompressible Navier-Stokes equation, impose slip/symmetry boundary conditions on Boundaries 1 and 4 (the left and right walls). Then, make the boundaries periodic. To impose periodic boundary conditions, set boundaries 1 and 4 as symmetry boundaries as shown in Figure 4.

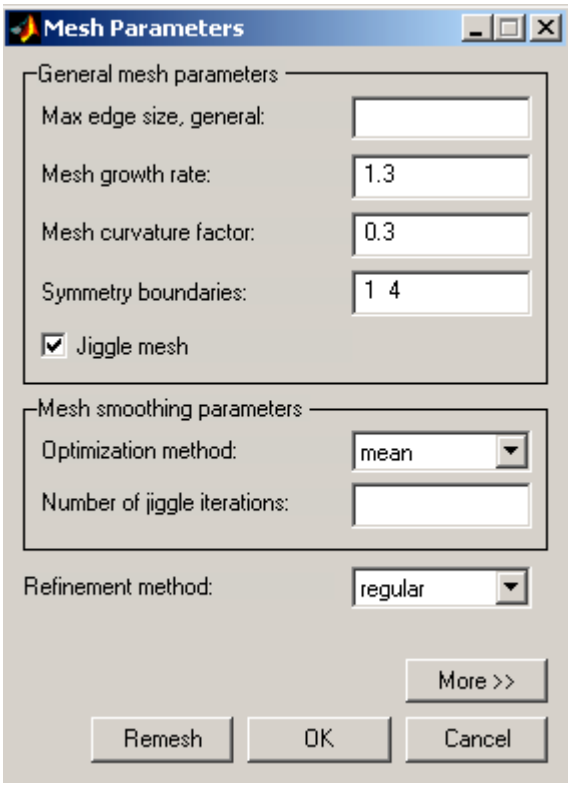

Figure 4. The symmetry boundaries are defined in the Mesh Parameters. This makes the two boundaries equivalent. The mesh is refined twice before the solution begins.

Then, select Boundary 1 from the h-tab in the Boundary Settings window and set the main diagonal to 1 and the other elements to 0 as shown in Figure 5.

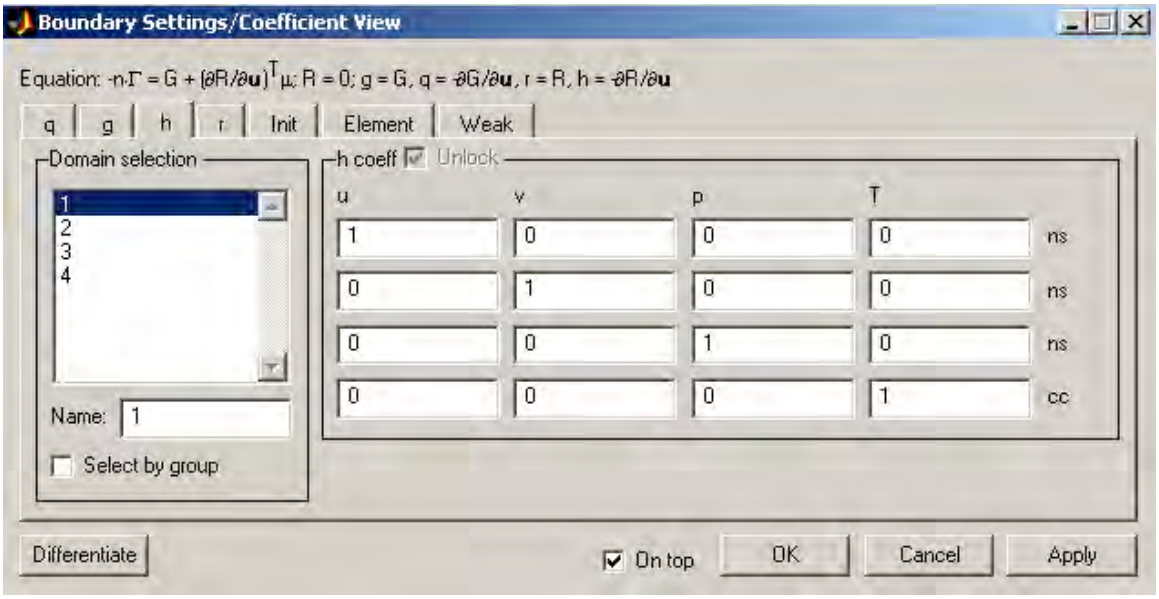

Figure 5. The first step in creating periodic boundary conditions is to select the h-tab in the Boundary Settings window for Boundary 1 and set the main diagonal to 1.

Next, the r-tab is selected so that the variables u, v, p, and T can be entered in order as shown in Figure 6.

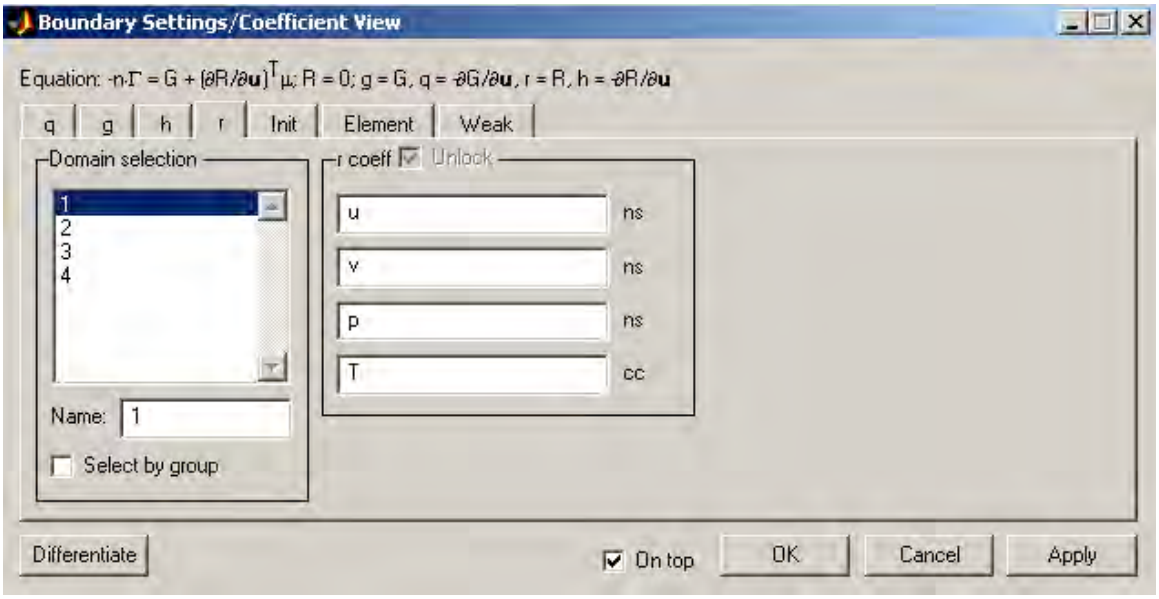

Figure 6. On the r-tab, the variables u, v, p, and T need to be entered as shown (all positive). This ends the specification for Boundary 1.

For Boundary 4, the main diagonal elements on the h-tab are set to -1, and the other elements are set to 0 as shown in Figure 7.

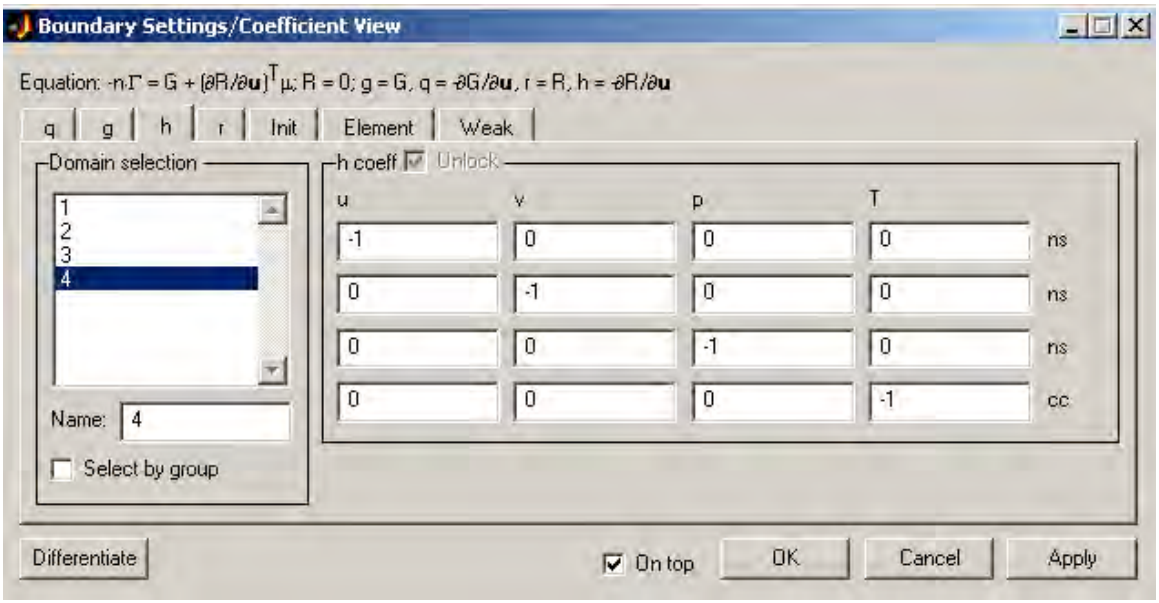

Figure 7. The second step in creating periodic boundary conditions is to select the h-tab in the Boundary Settings window for Boundary 4 and set the main diagonal to -1.

For Boundary 4, –u, -v, -p, and –T are entered in order on the r-tab as shown in Figure 8.

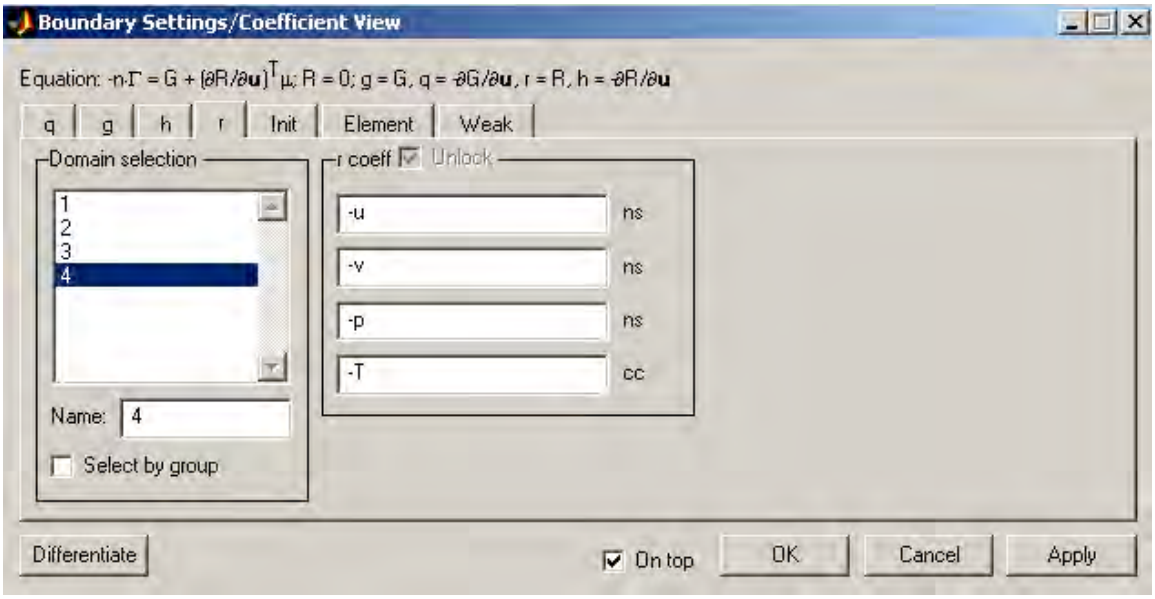

Figure 8. The variables u, v, p, and T need to be entered on the r-tab for Boundary 4 with negative signs in front of them. This ends the specification of periodic boundary conditions.

The no-slip condition is imposed on Boundaries 2 and 3 (the hot bottom plate and cold top plate). The Subdomain settings are given in Figure 9.

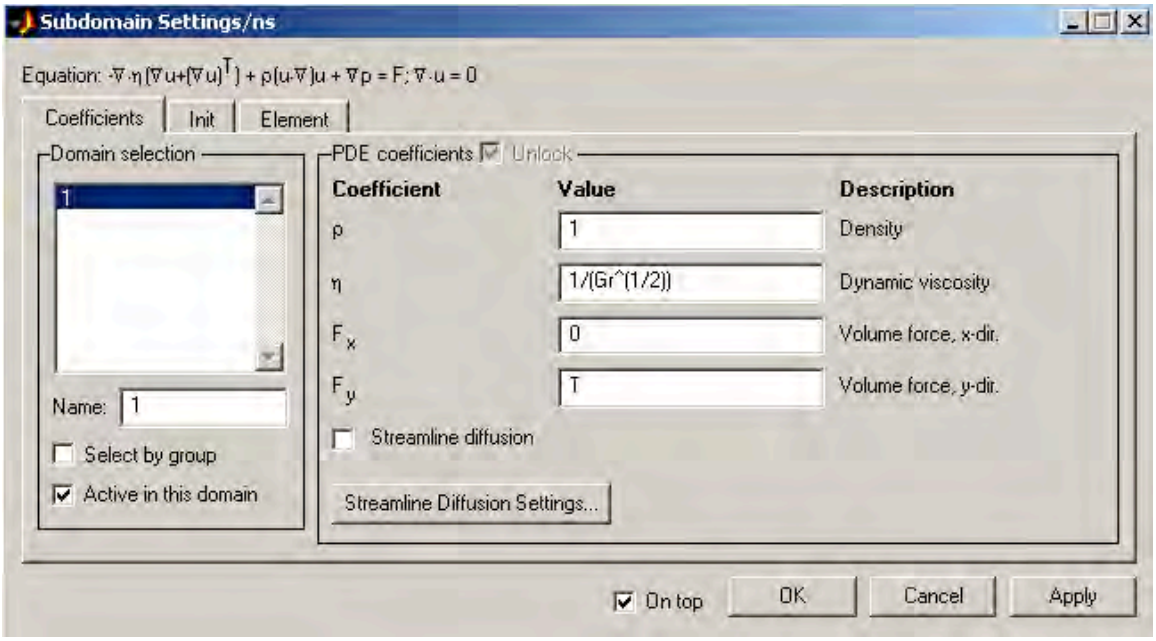

Figure 9. Subdomain settings for the Navier-Stokes equation. The Grashoff number is allowed to vary.

The pressure term does not have a coefficient in front of it. Thus, the coefficient $1/Gr^{1/2}$ cannot be entered into FEMLAB for it. Fortunately, this situation is only a minor annoyance rather than an impediment to obtaining a solution. For now, one can simply pretend that the pressure term is indeed divided by $Gr^{1/2}$. If one desires to translate from computer results to real life numbers for the pressure (and for the other variables u and v), one simply takes the pressure value from the computer and multiplies by $Gr^{1/2}$ first before doing anything else. Then, multiply by the definition of the pressure standard (or velocity standard) found in Appendix A. Alternatively, one can think of this situation as follows: Dividing the equations by the relevant dimensionless variables simply changes the definition of the pressure standard. The relative pressure drop between any two points in the simulation is the same no matter what the coefficient is in front of the pressure term in FEMLAB. The program does not know the pressure standard being used and does not care.

For the Convection and Conduction equation, Boundaries 1 and 4 are set as Insulation/Symmetry and then made periodic as described above. On Boundary 2, the temperature is set to 1. On Boundary 3, the temperature is set to 0. The Subdomain settings are given in Figure 10.

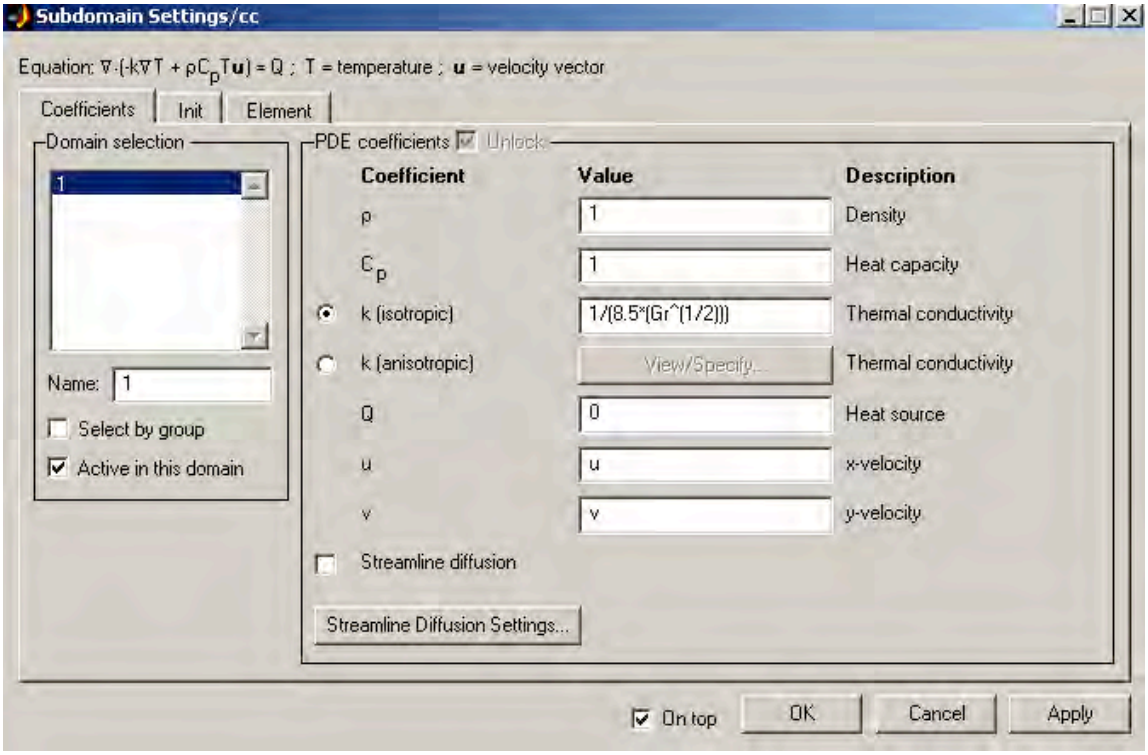

Figure 10. Subdomain settings for the Convection and Conduction equation. The Prandtl number is held constant at 8.5.

The pressure is under-specified. Thus, the Point Settings are changed in the manner shown in Figure 11.

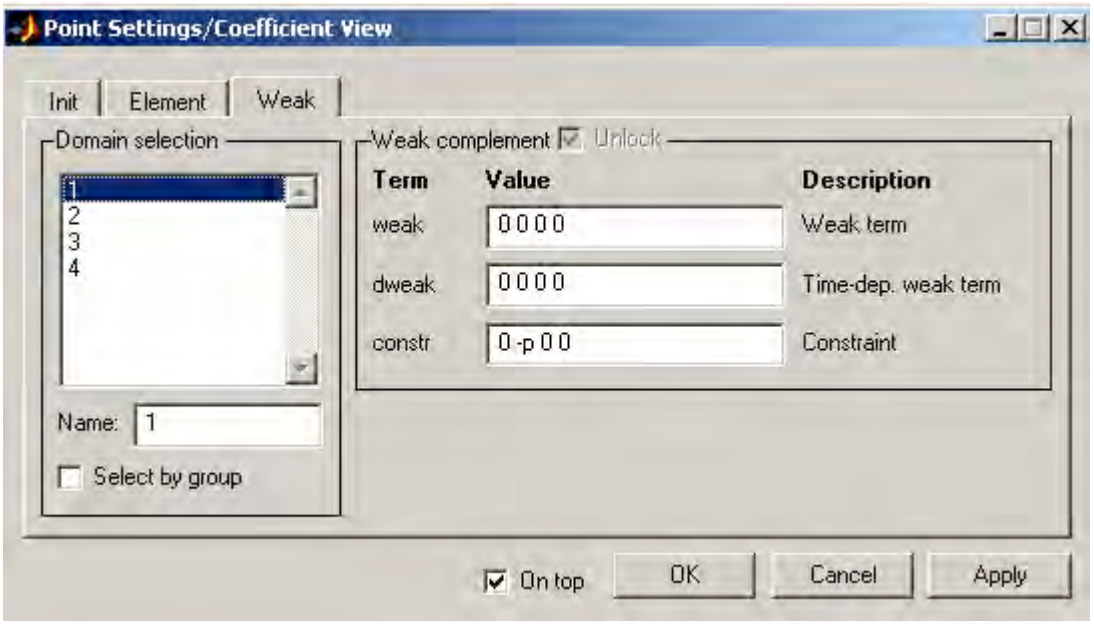

Figure 11. Point Settings for Point 1. One of the zeros in the Constraint field on the Weak tab is replaced with –p. The same procedure is performed for the other three points as well with the same zero being replaced for all four points.

Next, the Scaling of Variables is chosen as None on the Solve Parameters General tab. Now, define Gr as a coupling variable as shown in Figure 12.

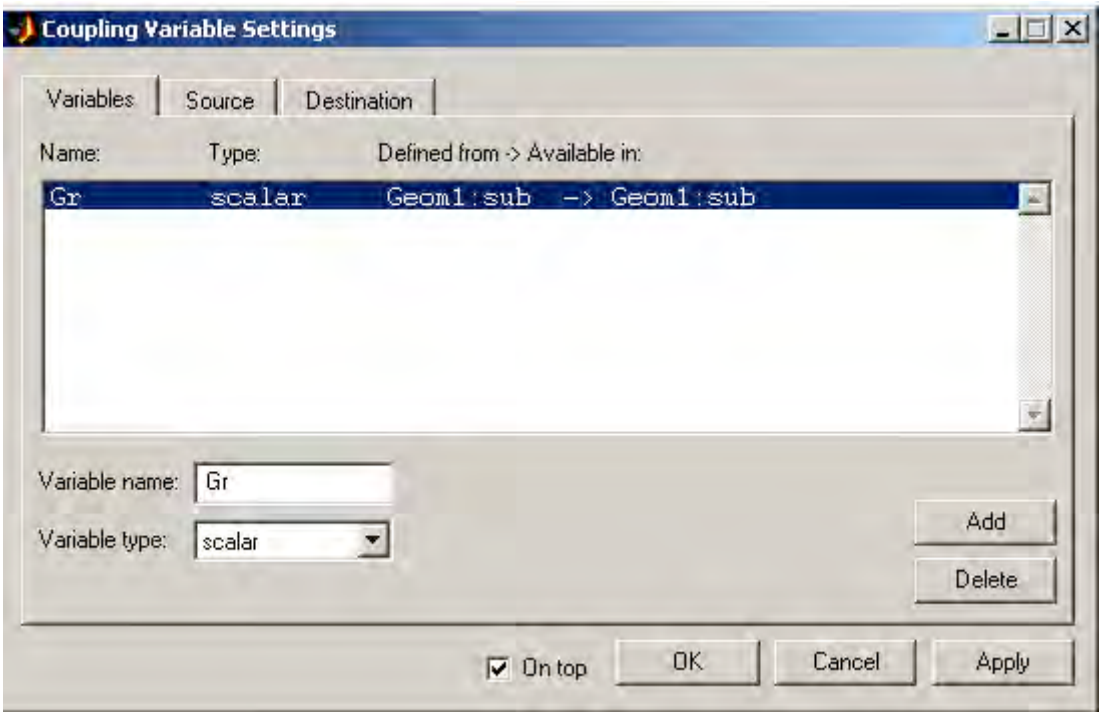

Figure 12. The symbol "Gr" is chosen to represent the Grashoff number. This set-up allows FEMLAB to solve for many different Grashoff numbers sequentially using the Parametric Solver.

The Parametric solution tab under Solve Parameters is set up to allow FEMLAB to solve the convective instability problem for Grashoff numbers of 50, 100, 150…550 all sequentially while using the previous solution as the initial guess for the next parameter value. The set-up is shown in Figure 13. Remember to select a Parametric solution on the General tab as well.

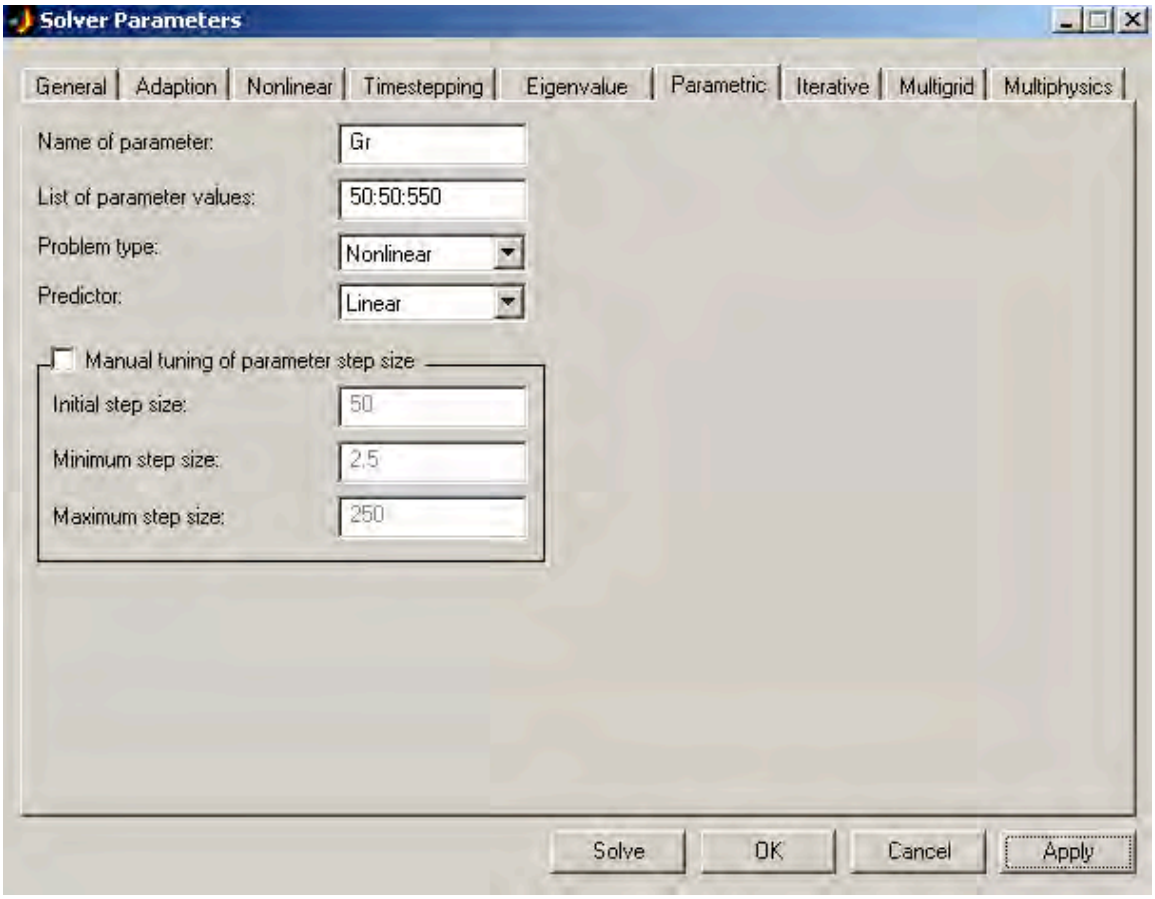

Figure 13. Solving for many different values of a variable using the Parametric Solver dramatically reduces the total solution time.

The simulation set-up is complete. There is no need to specify an initial velocity or perform any additional steps in Matlab.

Calculation of Nusselt number

The Nusselt number is calculated using

$$Nu = \frac{(normal\ total\ heat\ \ flux)\,\mathrm{Pr}\sqrt{Gr}}{4.5}$$

where the "normal total heat flux" is obtained from the computer using the Boundary Integration command. The length of the boundary is 4.5 units. Thus, the result of the integration along the boundary needs to be divided by the length of the boundary to obtain the heat flux. Also, multiplication by $\mathrm{Pr}\,\mathrm{Gr}^{1/2}$ is necessary because of the way in which the equations are entered into FEMLAB. For the details of the derivation, see Appendix B.

Results

Some of the plots obtained from FEMLAB are provided below.

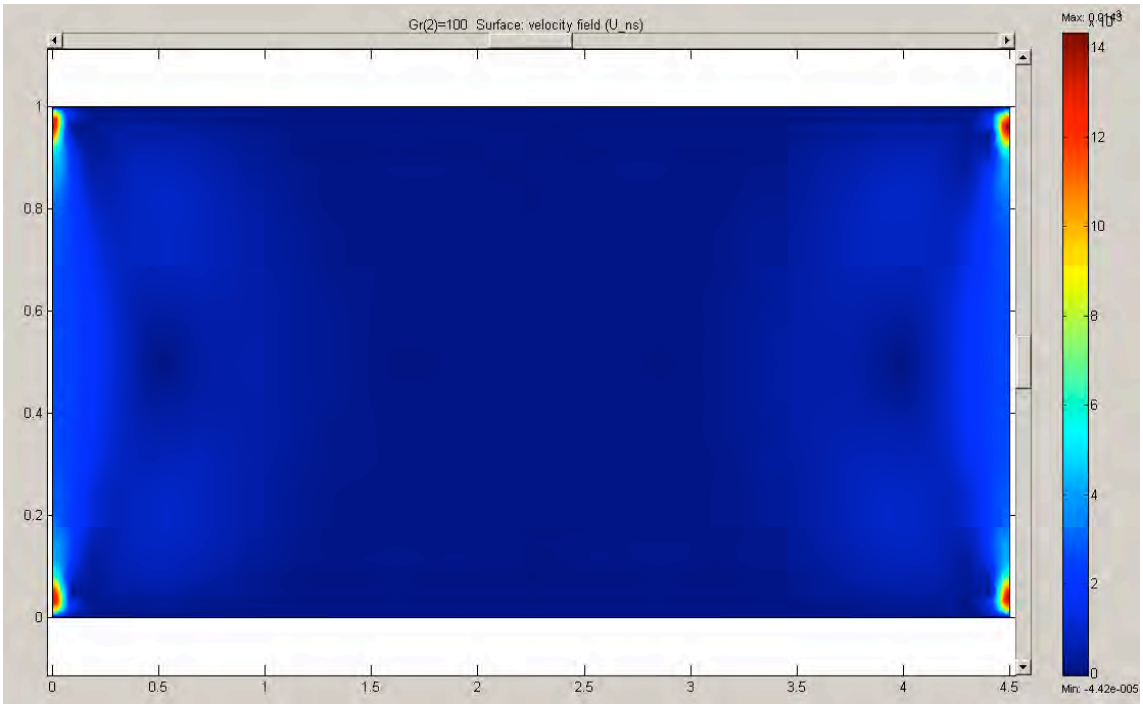

Figure 14. Surface velocity field plot for Gr = 100 (Ra = 850). There is very little fluid movement, and the maximum velocity is only 0.0143.

The fluid is just beginning to form convection cells for a Grashoff number of 200 (Rayleigh number of 1700) as if preparing for convection as seen in Figure 15.

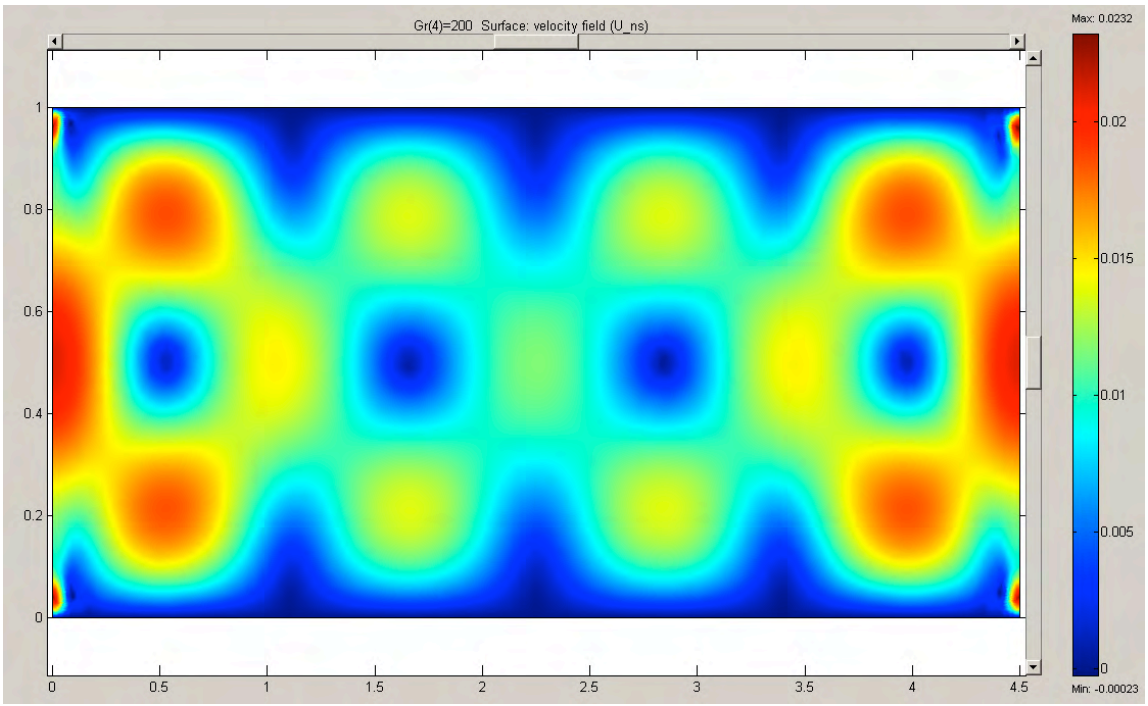

Figure 15. Surface velocity field plot for Gr = 200 (Ra = 1700) just before the onset of convection. Most of the fluid is still moving slowly. The maximum velocity is 0.0232.

Once Ra_c has been surpassed, the fluid begins to circulate.

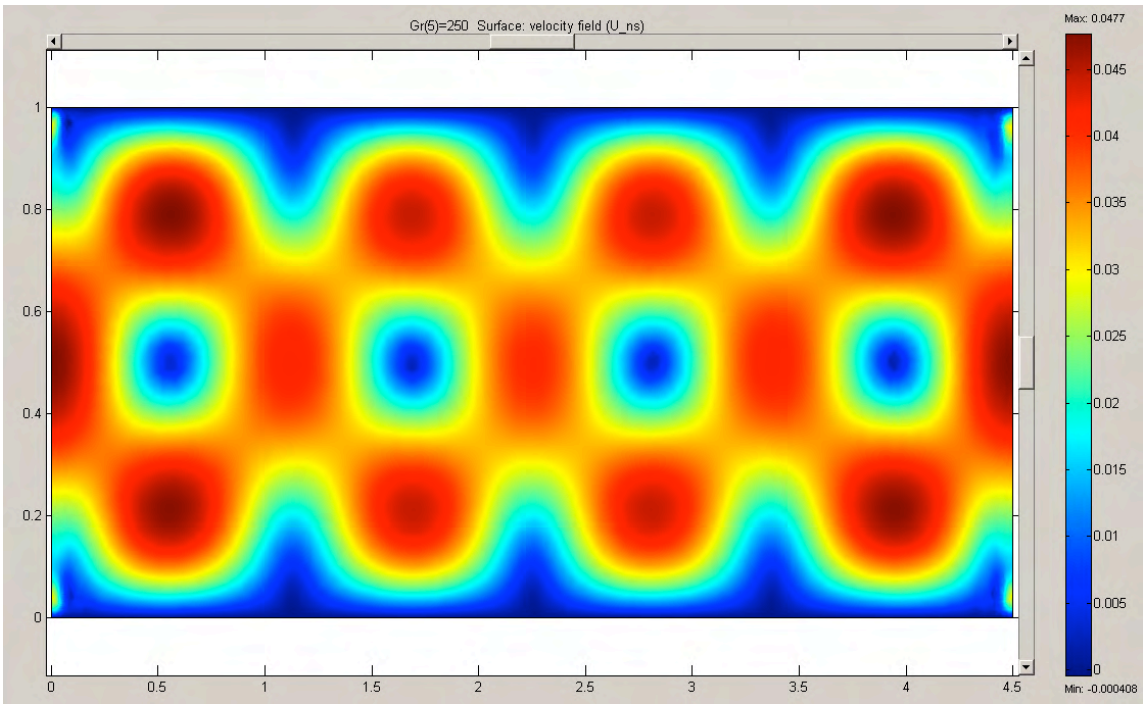

Figure 16. Surface velocity field plot for Gr = 250 (Ra = 2125). The onset of convection has occurred. Most of the fluid is moving at the maximum velocity of 0.0477.

For higher Grashoff numbers, the surface velocity field plot remains essentially the same, but the maximum velocity continues to increase as seen in Figure 17.

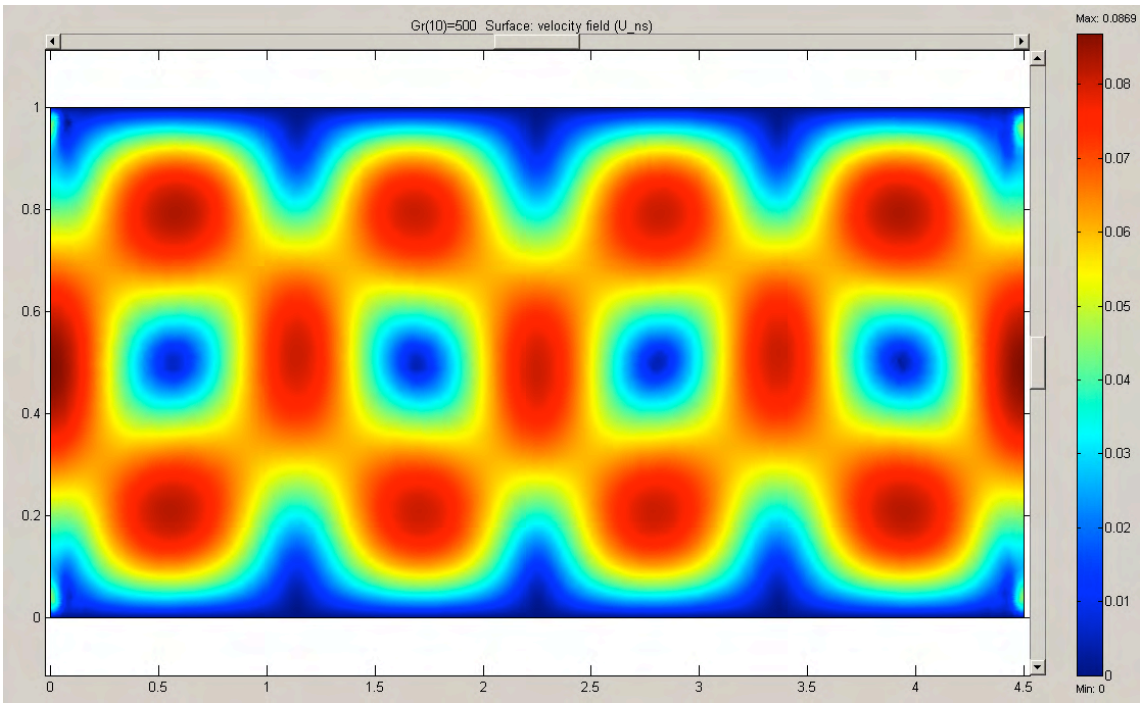

Figure 17. Surface velocity field plot for Gr = 500 (Ra = 4250). The maximum velocity has increased to 0.0869.

Let's study the case when the Grashoff number is 500.

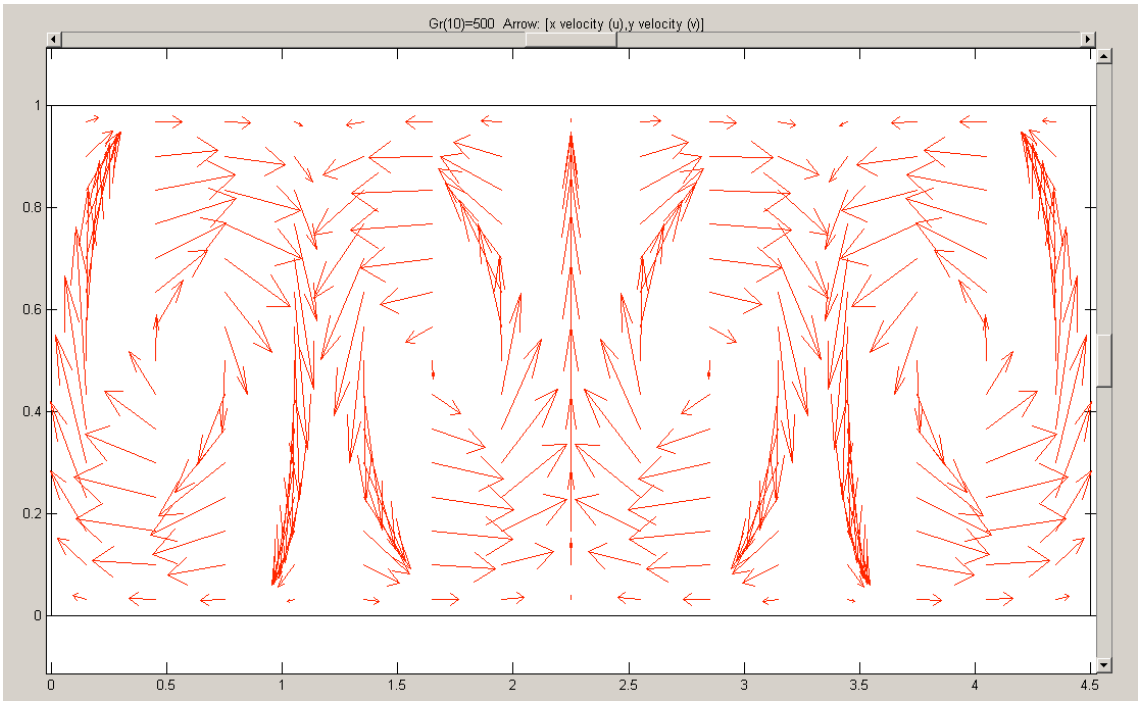

Figure 18. Arrow plot of velocity vectors for Gr = 500 (Ra = 4250). The fluid moves up the center and splits into two streams that head left and right. The fluid cools and then falls back down again.

The width of the convection cells is most easily seen by examining a flow plot.

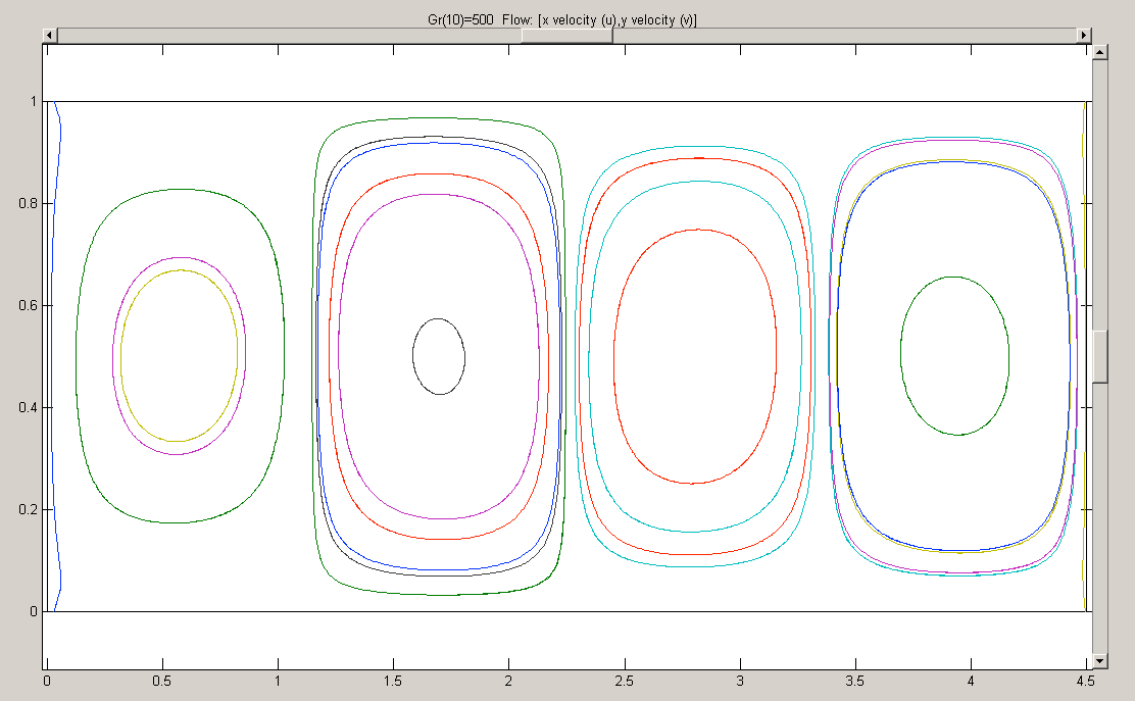

Figure 19. Flow plot of velocity for Gr = 500 (Ra = 4250). The height of the cells vary from around 0.6 to almost 1.0 units.

Now, examine the temperature profile. The original profile was linear as seen in Figure 20.

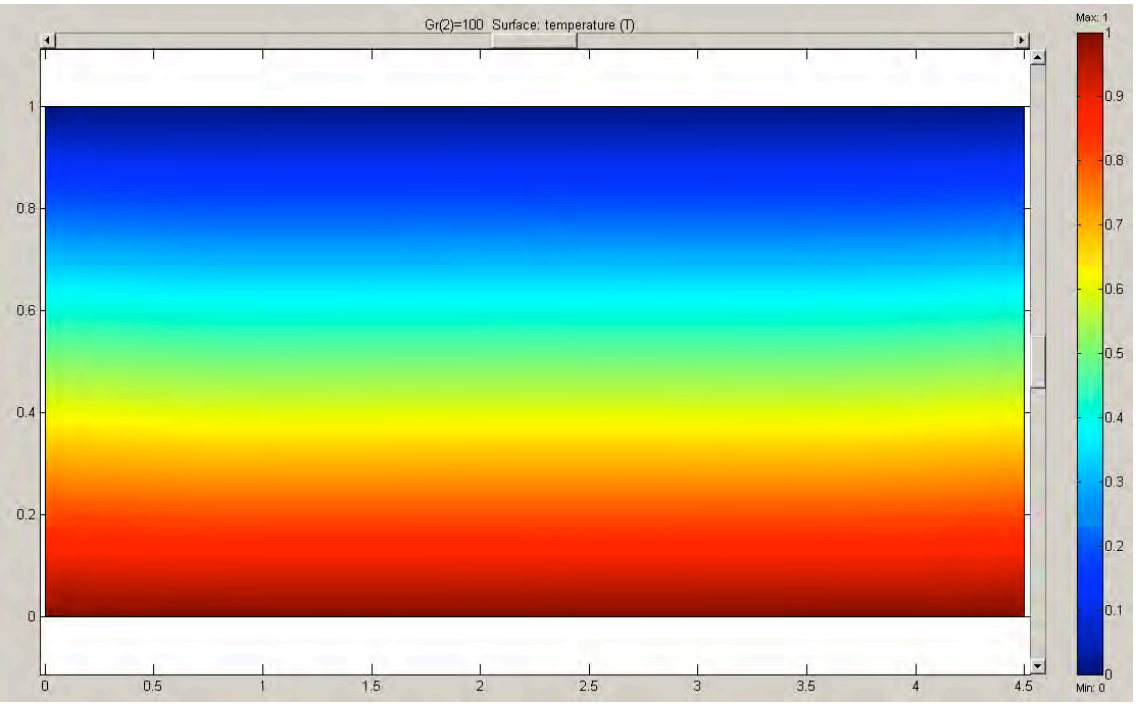

Figure 20. Surface plot of temperature for Gr = 100 (Ra = 850). Before the onset of convection, the temperature profile is essentially linear.

However, the temperature profile after the onset of convection is drastically non-linear as shown in Figure 21.

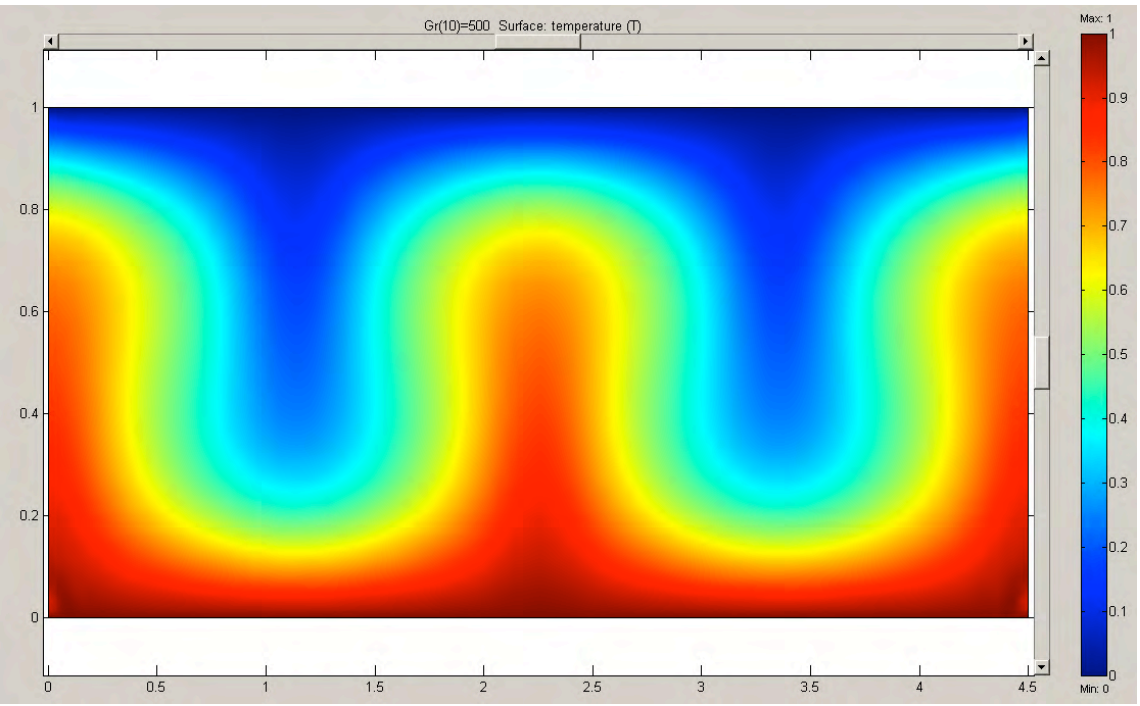

Figure 21. Surface plot of Temperature for Gr = 500 (Ra = 4250). The fluid that is forced to travel upward maintains its hot temperature past the 0.6 mark in the y-direction.

An unstable branch of the solution is identified by running the simulation differently. To obtain the points on the unstable branch, the parametric solver is used to solve for values of the Grashoff number of 100, 300, and 500. Apparently, taking such large parameter steps in FEMLAB leads to the unstable branches. The results of these three simulations are presented in Figures 22-24.

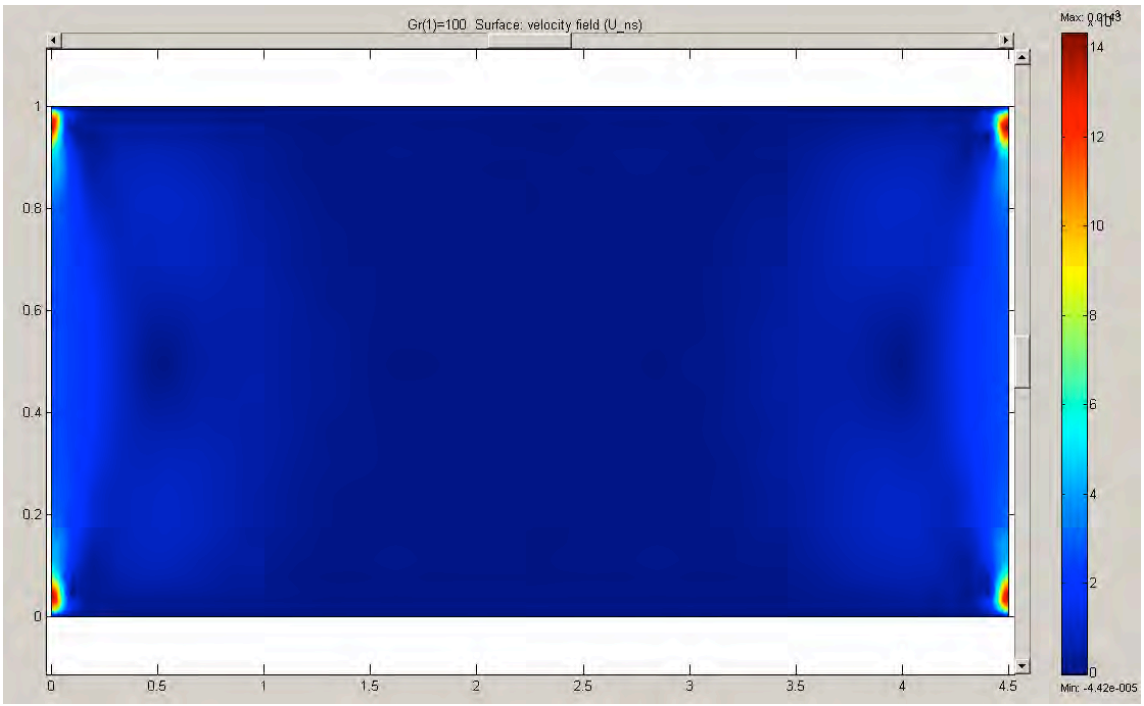

Figure 22. Surface plot of velocity field for Gr = 100 (Ra = 850) for the unstable branch. This solution served as the precursor for the other unstable branch solutions. It has the same maximum velocity as the corresponding solution on the stable branch, and there is no discernable difference between them.

When the Grashoff number is increased to 300, an entirely different solution is obtained from the corresponding one on the stable branch even though they both started from the same solution.

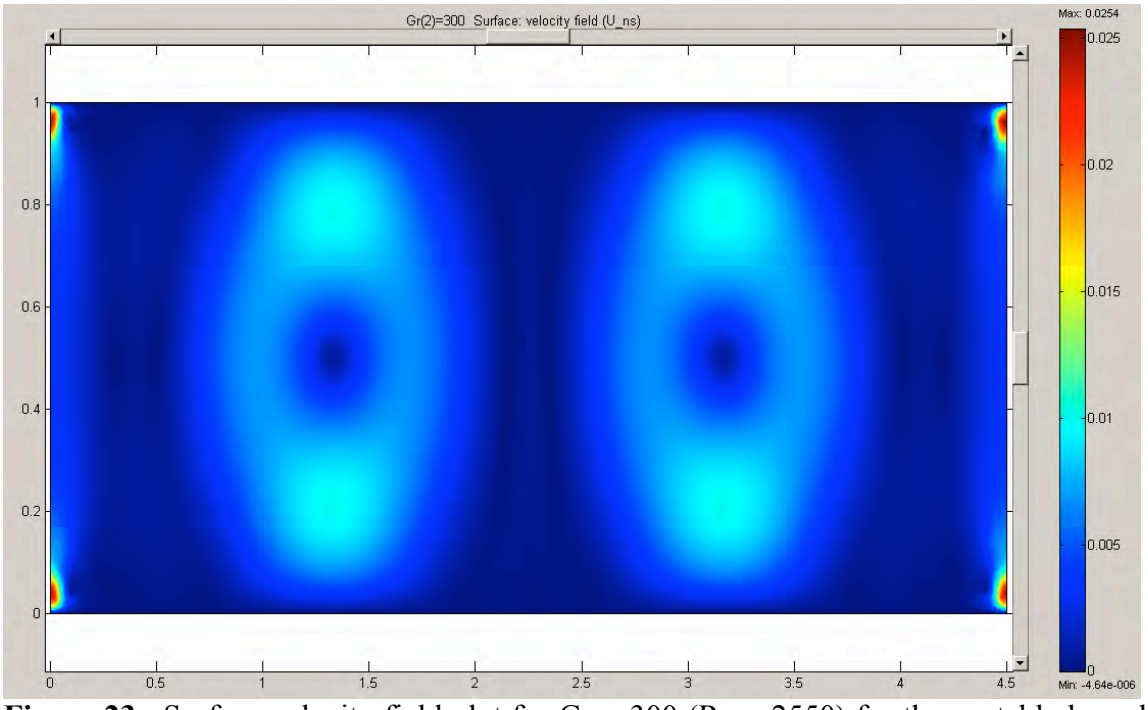

Figure 23. Surface velocity field plot for Gr = 300 (Ra = 2550) for the unstable branch. From the lack of red coloring on the plot, it appears that convection has not started yet.

When the Grashoff number is increased to 500, the pattern seen in the previous surface plot is seen to have developed more.

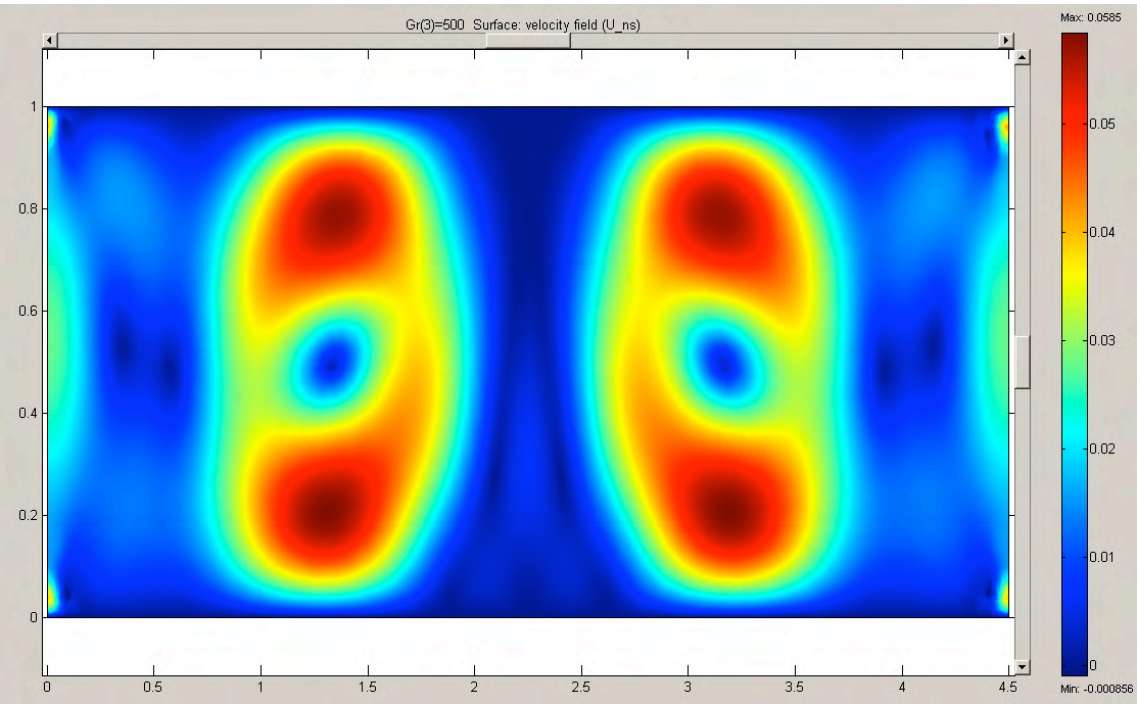

Figure 24. Surface velocity field plot for Gr = 500 (Ra = 4250) for the unstable branch. Portions of the plot appear red, indicating that at least some of the fluid is now moving at the maximum velocity. The final determination of whether or not convection has started is still the value of the Nusselt number, though.

The dimensionless normal total heat flux and the maximum velocity are extracted from the simulation results. The heat flux is obtained through boundary integration along the top and bottom plates, and the maximum velocity is read from the plots. The Nusselt and Rayleigh numbers are calculated and plotted in Microsoft Excel. The results are shown below in Table 1 and Figure 25.

Table 1. Nusselt number as a function of Rayleigh number. The data is taken from the FEMLAB simulations.

Gr	Ra	Stable Branch Normal Total Heat Flux	Nu	Unstable Branch Normal Total Heat Flux	Nu
50	425	0.074963	1.001		
100	850	0.053082	1.003	0.053082	1.003
150	1275	0.043435	1.005		
200	1700	0.039122	1.045		
250	2125	0.043858	1.310		
300	2550	0.04648	1.521	0.031036	1.015
350	2975	0.047625	1.683		
400	3400	0.048012	1.814		
450	3825	0.047994	1.923		
500	4250	0.047755	2.017	0.030242	1.277
550	4675	0.047394	2.099		

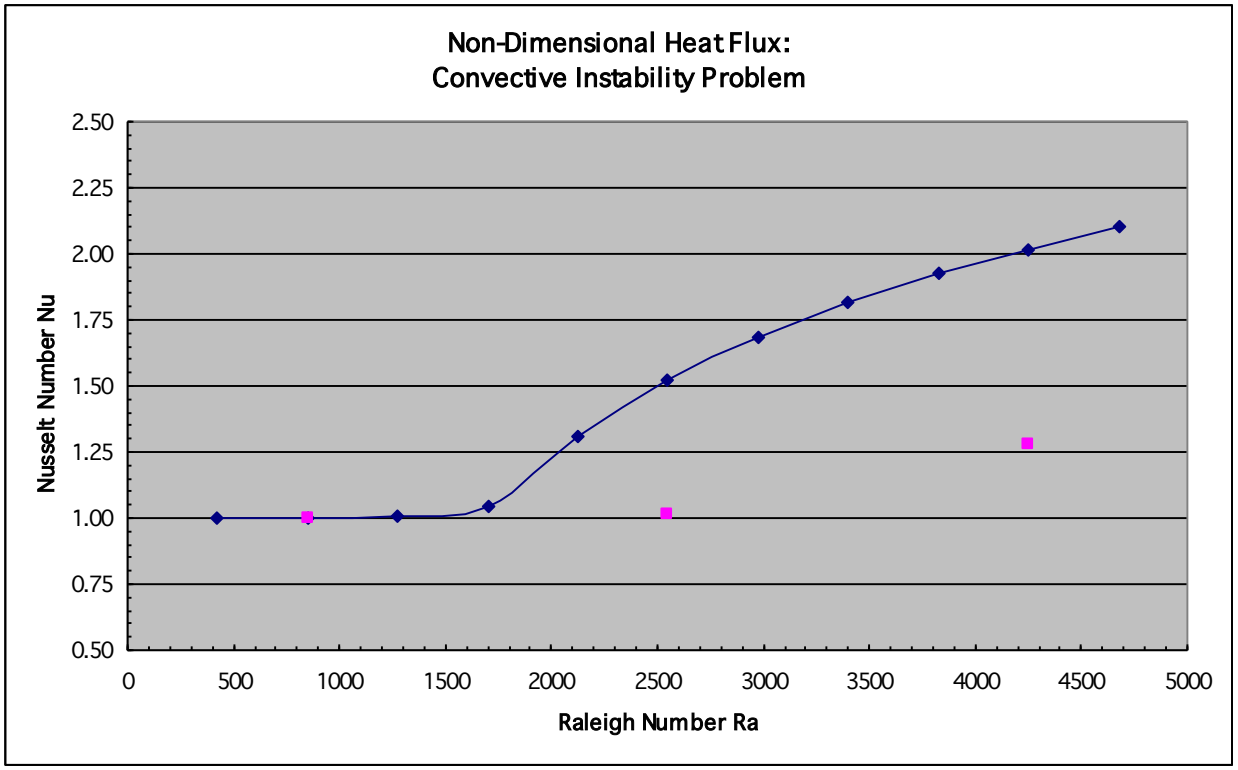

Figure 25. Plot of data obtained from FEMLAB. The main branch of the solution is the solid line, which appears to have the exact same shape as the expected line from Figure 3. The Nusselt number for the unstable branch begins to differ from one around the expected value. The three pink squares represent the points on the unstable branch. The Nusselt number for the unstable branch remains essentially one even for the case of Gr = 300 (Ra = 2550).

Discussion

The FEMLAB curve from Figure 25 is virtually identical to the experimental curve from Figure 3. The onset of convection in the FEMLAB simulation seems to occur a little before the theoretical value of $Ra_c = 1707.762$, but this abnormality is most likely caused by the energy balance convergence error. The difference between the heat flux leaving the bottom plate and the heat flux entering the top plate is about 2-3%.

Conclusions

Based on the results, convective instability can be successfully modeled using FEMLAB. In addition, at least one unstable branch of the solution seems to exist, and FEMLAB is capable of finding it.

Recommendations

The following future work is recommended to see if FEMLAB can model it:

- A concentration gradient should be added to the simulation.
- A 3-dimensional simulation for a rigid boundary on the bottom and a free surface on top should be created to see if the hexagonal cell structure is observed and if the value of Ra_c matches the value expected from theory for this case.
- A thermal diffusion term should be added to determine its effect on the stability of the system.
- The unstable branch(es) of the solution should be further identified, studied, and documented.
- The graph should be extended to include much higher Rayleigh numbers.

Literature Cited

1. Day, Charles. "Thermal Gradients Can Boost the Local Concentration of DNA in Solution." Physics Today. February 2003.

2. Bird, R. Byron, Edwin N. Lightfoot and Warren E. Stewart. Transport Phenomena. John Wiley and Sons: New York, 1960.

3. http://astron.berkeley.edu/~jrg/ay202/node135.html

This site is maintained by James R. Graham of the Astronomy Department at Berkeley University. This web page is part of his Astronomy 202 class notes. This site is considered credible because his numbers were verified by other sources.

4. Chandrasekhar, S. Hydrodynamic and Hydromagnetic Stability. Clarendon Press: Oxford, 1961.

5. Berg, John C. Surface and Colloid Science. Department of Chemical Engineering, University of Washington: Seattle, 2003.

References

Dewitt, David P. and Frank P. Incropera. Fundamentals of Heat and Mass Transfer, 5th edition. John Wiley and Sons: New York, 2002.

Snyder, Suzanne M., Tahir Cader, and Bruce A. Finlayson. "Finite Element Model of Magnetoconvection of a Ferrofluid." Journal of Magnetism and Magnetic Materials. 2003.